

ESTIMATION OF GRAVIMETRIC VEGETATION MOISTURE IN THE WESTERN UNITED STATES USING A MULTI-SENSOR APPROACH

David Chaparro¹, Thomas Jagdhuber^{1,2}, Maria Piles³, François Jonard⁴, Mercè Vall-llossera⁵, Adriano Camps^{5,6}, Carlos López-Martínez⁵, Anke Fluhrer^{1,2}, Roberto Fernández-Morán³, Martin J. Baur⁷, Andrew F. Feldman⁸, Dara Entekhabi⁹

¹German Aerospace Center, Microwaves and Radar Institute, Münchener Strasse 20, 82234 Wessling, Germany

²Institute of Geography, University of Augsburg, Alter Postweg 118, 86159 Augsburg, Germany

³Image Processing Lab, Universitat de València, 46980 València, Spain

⁴Earth Observation and Ecosystem Modelling Laboratory, SPHERES Research Unit, Université de Liège (ULiège), 4000 Liège, Belgium

⁵CommSensLab, Department of Signal Theory and Communications, and Institut d'Estudis Espacials de Catalunya, Universitat Politècnica de Catalunya (UPC), 08034 Barcelona, Spain

⁶ASPIRE Visiting International Professor, UAE University, CoE, POBox 15551, Al Ain, UAE

⁷University of Cambridge, Department of Geography, Downing Place, CB2 3EN Cambridge, UK

⁸NASA Postdoctoral Program, Biospheric Sciences Laboratory, NASA Goddard Space Flight Center, Greenbelt, MD 20771, USA

⁹Civil and Environmental Engineering, Massachusetts Institute of Technology, Cambridge, MA 02139 USA

ABSTRACT

Vegetation optical depth (VOD) depends on the water, structure, and biomass of vegetation. Here, we propose a multi-sensor approach to isolate the water component from the VOD and to retrieve gravimetric vegetation moisture (m_g) in the western United States. The approach estimates VOD from radar and LiDAR data and minimizes the differences between these estimates and SMAP/AMSR2 VOD observations. This minimization allows to obtain the best fitting value of m_g with help of a dielectric model. Results are consistent both in space (drier vegetation in arid areas) and time (drier vegetation in drier months). The m_g estimates are in the same range than in situ m_g data, with some underestimation (bias ~ -0.07 kg/kg). Statistical results are reasonable ($r \sim 0.45$, $RMSE \leq 0.10$ kg/kg), yet the different spatial and temporal representation of in situ and remote measurements have an impact in the direct comparisons. Our results highlight the potential for developing new vegetation moisture datasets based on VOD decomposition.

Index Terms— Vegetation moisture, passive microwaves, vegetation optical depth, LiDAR, Sentinel-1.

1. INTRODUCTION

Passive microwave satellite missions allow for the retrieval of the vegetation optical depth (VOD), a parameter which accounts for the degree of attenuation of the soil and vegetation emissions in microwave frequencies as they cross

the vegetation canopy. The VOD is directly related to the vegetation water content (VWC), which is central to the analysis of the soil-plant-atmosphere continuum [1] and ultimately understanding plant responses to droughts. However, since the VOD is a function of water, dry biomass, and structure of the vegetation, the VOD-derived VWC estimates depend on biomass/structure properties. Indeed, the VWC is measured in units of mass of water by ground area (kg/m^2), not informing on the real hydric status of plants (e.g., a forest contains more water than a grassland because it has more biomass). To overcome these limitations, it is essential to isolate the water component from the VOD signal. In that sense, the leaf area index (LAI) has been applied in [2] to account for the canopy structure component and has shown that merging LAI and VOD data improves the estimates of live fuel moisture content (LFMC; $\text{kg}_{\text{water}} / \text{kg}_{\text{dry biomass}}$) at a global scale [2]. Also, it has been demonstrated that merging Sentinel-1 radar backscatter information with optical data from Landsat-8 leads to improved LFMC estimates in the western United States [3].

These results have shown the benefits of exploiting multi-sensor synergies to enhance vegetation moisture estimates based on statistical regression [2] and neural networks [3]. Nevertheless, physics-based, analytical algorithms (e.g., considering dielectric and attenuation models in vegetation) have been proposed only in preliminary studies. In that sense, in [4] and [5] a microwave-LiDAR synergy was used to disentangle the water component from the VOD with help of such models. Here, we rely on a similar synergetic approach to estimate the vegetation moisture in

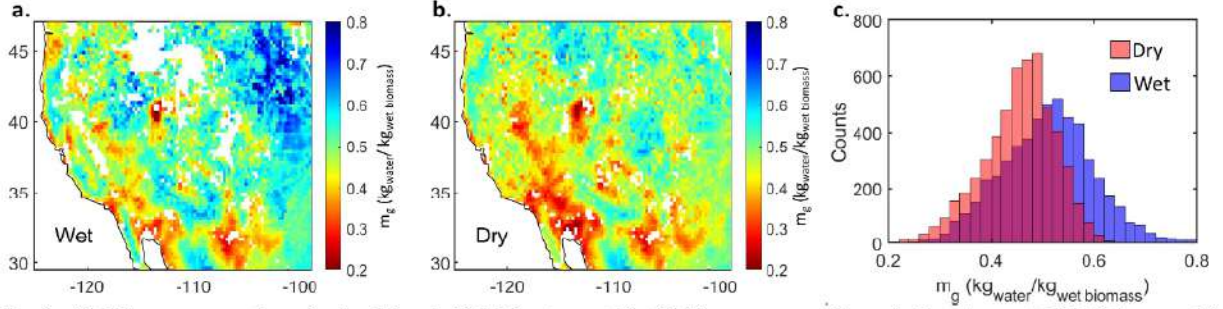


Fig. 1. (a) Time-averaged m_g during March 2017 (wet month); (b) Time-averaged m_g during August 2017 (dry month); (c) histogram comparing wet and dry months. In a and b, blank areas are due to snow and/or non-vegetated pixels. In this figure, m_g retrievals are based on X-band VOD. Similar results are obtained at L- and Ku-bands.

gravimetric units (m_g ; $\text{kg}_{\text{water}}/\text{kg}_{\text{wet biomass}}$) in the western United States with three clear goals: 1) adapt the m_g retrieval approach to different microwave frequencies (L-, X- and Ku-bands) and dielectric models, 2) analyze m_g spatio-temporal estimates over the Western United States, and 3) compare satellite-based m_g with available in situ data. The study spans from April 2015 to December 2018.

2. DATA AND METHODS

The multi-sensor approach for m_g retrieval relies on three data products: VOD, radar backscatter information, and vegetation canopy height. In this work we use the Soil Moisture Active-Passive (SMAP) VOD to account for microwave attenuation at L-band. The SMAP VOD product [6] is retrieved through the multi-temporal dual channel algorithm (MT-DCA; [7]). We also use VOD data at X- and Ku-bands from the Advanced Microwave Scanning Radiometer 2 (AMSR2; [8]). Second, to account for the biomass and structure components, we apply radar

backscatter information from Sentinel-1 [9] and vegetation canopy height (VH) data from [10]. The latter is based on lidar measurements from the Global Ecosystem Dynamics Investigation (GEDI) sensor, and Sentinel-2 data. All datasets are aggregated at a 0.25° grid to match the VOD product gridding.

The proposed algorithm is structured in three steps. First, the VOD is modelled according to [11] as a function of a radar vegetation index (RVI), an approximation to the shape of leaf inclusions (see [12]; random needles are chosen here), the VH information, and the dielectric constant of vegetation (ϵ_{veg} , which is the unknown to be solved). This model is calibrated for different RVI conditions. Second, the best ϵ_{veg} value is found through the minimization of the difference between the modeled VOD and the SMAP VOD data, at a daily basis. Third, using the dielectric models in [13] and [14], the m_g value corresponding to the chosen ϵ_{veg} is retrieved. More details on the algorithm proposed are available in [4], [5] and [12].

m_g retrievals are compared to available in situ data provided in [15]. The in situ data are destructive samples

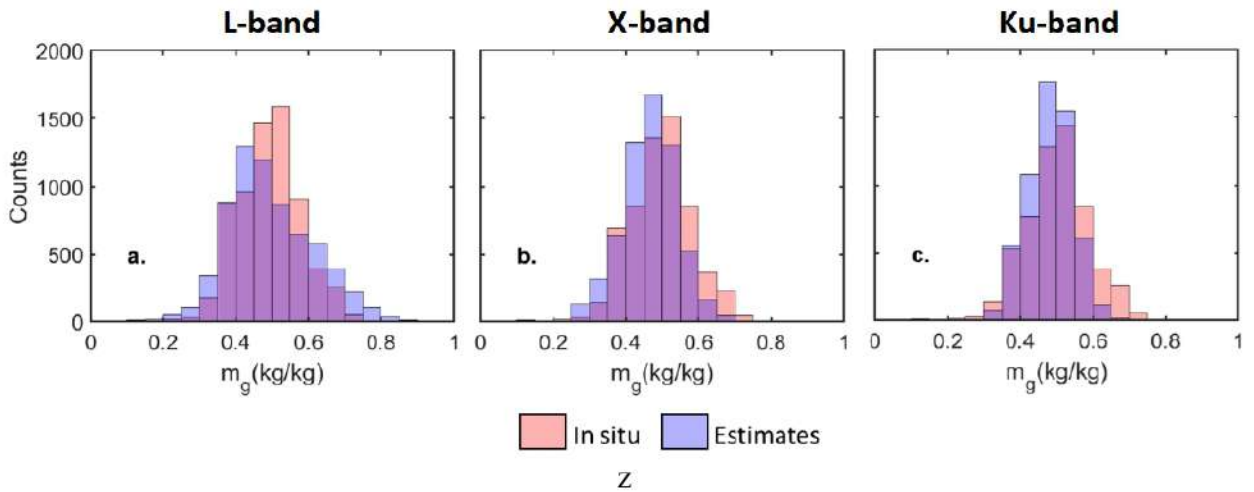


Fig. 2. Comparison between in situ (pink) and estimated (blue) m_g for (a) L-band, (b) X-band and (c) Ku-band.

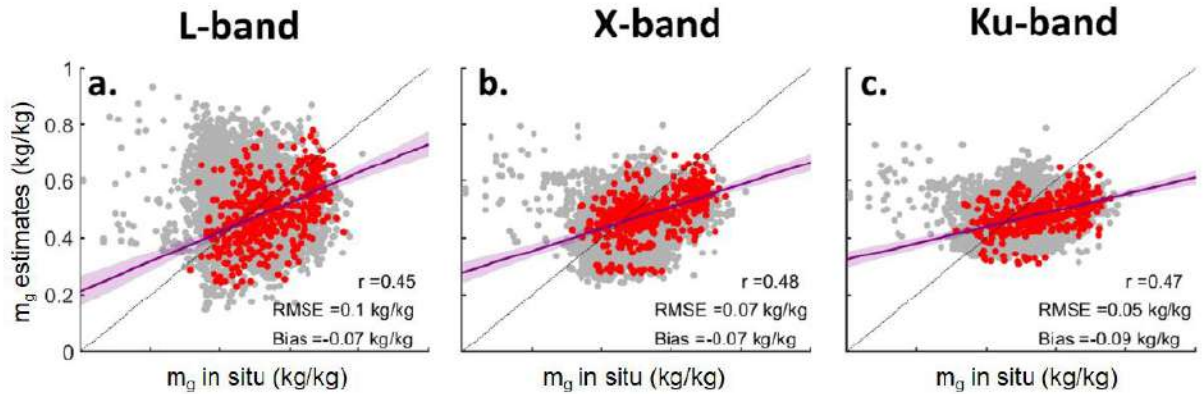


Fig. 3. Relationship between the in situ m_g measurements and the m_g estimates, using each pair of in situ – estimates during the study period. The m_g estimates are based on the dielectric model from [13]. Statistics are computed for the 29 homogeneous stations (>700 samples; red dots). Grey dots indicate the rest of samples over the study region (non-homogeneous pixels). Three frequency bands are studied: (a) L-band, (b) X-band, and (c) Ku-band.

which are weighed fresh, oven-dried and reweighed to determine dry matter mass. With this information, the Live Fuel Moisture Content (LFMC; in mass units of water per dry biomass) is determined, and then transformed to m_g ($m_g = 1/(1+LFMC)$; see [16]). In situ m_g data are obtained at different times in the year and are compared to the nearest overpass of AMSR2 and SMAP. The comparison is focused on pixels with homogenous land cover (to reduce the representativeness error due to scaling mismatch) and with enough number of in-situ samples. The criteria are: (i) all the species measured in situ must match the dominant land cover in the pixel, according to the ESA-CCI Land Cover map [17]; (ii) the Gini-Simpson Index (GSI), which indicates the homogeneity of land cover in the pixel [18], is <0.5 (i.e., land cover is homogeneous); (iii) the coefficient of variation of the NDVI in the 500-m area surrounding the in situ samples, which is a measure provided by [15], is <0.3 ; and (iv) the number of samples of the in situ station is ≥ 10 . Finally, 29 stations with more than 700 in situ measurements remain for validation.

3. RESULTS AND DISCUSSION

The resulting maps show the time-average m_g for a wet month (March 2017; Fig. 1a) and a dry month (August 2017; Fig. 1b). The spatial distribution of the results depicts, as expected, how southernmost regions (arid areas) have drier vegetation conditions. The histogram in Fig. 1c confirms the higher vegetation moisture in the wet period. Results also show that the retrieved m_g values based on all frequency bands fit the ranges of the in situ measurements, with some underestimation (Fig. 2).

Figure 3 shows the direct comparison of in situ and remotely sensed m_g estimates. Pearson's correlation is moderate and similar at all bands (0.45 to 0.48). The bias is also similar among bands, and confirms the underestimation

observed in Fig. 2 (-0.07 kg/kg to -0.09 kg/kg). The RMSE decreases with increasing frequency (from 0.1 kg/kg at L-band, to 0.07 kg/kg at X-band, and to 0.05 kg/kg at Ku-band). This trend is expected because L-band captures the vegetation conditions from the larger parts of the canopy (trunks and stems/branches), while in situ measurements are taken from the top leaves and only thin branches of the canopy [2,15]; the latter are more closely representative of the vegetation constituents contributing to C and X-bands emissions. Also, higher frequencies are more appropriate to measure vegetation properties in short vegetation, because they have lower penetration capacity [19], which dominates the region. All results presented in the figures are based on the dielectric model described in [13]. The comparison with [14] shows similar results, but with increased error and more negative bias (L-band: RMSE = 0.1 kg/kg, bias = -0.09 kg/kg; X-band: RMSE = 0.11 kg/kg, bias = -0.1 kg/kg). The model in [14] is not available at Ku-band. For both models, the reported correlation, error, and bias values are impacted by the spatial and temporal scale mismatch between in situ and satellite measurements and should be taken with caution.

Overall, the reported results show for the first time (to the authors' knowledge) a direct retrieval of gravimetric vegetation moisture based on the isolation of the water component from the VOD signal using a multi-sensor, multi-frequency, and attenuation-based approach. These results, thus, open the path for an enhanced capability of retrieving vegetation moisture conditions by using simple analytical models on physics basis. The fact that results at all frequencies show moderate correlations with medium to low error suggests that the different frequency bands could provide vegetation moisture retrievals for different canopy layers. This could have large applicability on vegetation ecology, fire prevention, or the study of land-atmosphere interactions. Future missions, such as the Copernicus Imaging Microwave Radiometer (CIMR; cimr.eu), will be

well suited to apply this approach using multiple microwave frequencies.

4. REFERENCES

- [1] A.F. Feldman, D.J.S. Gianotti, A.G. Konings, K.A. McColl, R. Akbar, G.D. Salvucci, D. Entekhabi. "Moisture pulse-reserve in the soil-plant continuum observed across biomes," *Nature Plants*, 4(12), pp. 1026-1033. 2018.
- [2] M. Forkel, L. Schmidt, R. M. Zotta, W. Dorigo, & M. Yebra. "Estimating leaf moisture content at global scale from passive microwave satellite observations of vegetation optical depth," *Hydrology and Earth System Sciences*, 27(1), pp. 39-68. 2023.
- [3] K. Rao, A. P. Williams, J.F. Flefil, & A. G. Konings. "SAR-enhanced mapping of live fuel moisture content," *Remote Sensing of Environment*, 245, 111797. 2020.
- [4] A. Fink, T. Jagdhuber, M. Piles, J. Grant, M. Baur, M. Link, D. Entekhabi. "Estimating gravimetric moisture of vegetation using an attenuation-based multi-sensor approach," *IGARSS 2018*, IEEE, pp. 353-356. 2018.
- [5] T. Meyer, T. Jagdhuber, M. Piles, A. Fink, J. Grant, H. Vereecken, F. Jonard. "Estimating gravimetric water content of a winter wheat field from L-band vegetation optical depth," *Remote Sensing*, 11(20), p. 2353. 2019.
- [6] A. Feldman, A. G. Konings, M. Piles, & D. Entekhabi. (2021). The Multi-Temporal Dual Channel Algorithm (MT-DCA) (Version 5) [Data set]. Zenodo. <https://doi.org/10.5281/zenodo.5619583>
- [7] A. G. Konings, M. Piles, K. Rötzer, K. A. McColl, S. K. Chan & D. Entekhabi, D. "Vegetation optical depth and scattering albedo retrieval using time series of dual-polarized L-band radiometer observations," *Remote Sensing of Environment*, 172, 178-189. 2016.
- [8] L. Moesinger, W. Dorigo, R. De Jeu, R. Van der Schalie, T. Scanlon, I. Teubner & M. Forkel. (2019). The Global Long-term Microwave Vegetation Optical Depth Climate Archive VODCA (1.0) [Data set]. Zenodo. <https://doi.org/10.5281/zenodo.2575599>
- [9] NASA National Snow and Ice Data Center Distributed Active Archive Center. SMAP/Sentinel-1 L2 Radiometer/Radar 30-Second Scene 3 km EASE-Grid Soil Moisture V003. Available at: https://cmr.earthdata.nasa.gov/search/concepts/C1931663473-NSIDC_ECS.html. Last accessed: 30-09-2022.
- [10] N. Lang, N. Kalischek, J. Armston, K. Schindler, R. Dubayah, J.D. Wegner, "Global canopy height regression and uncertainty estimation from GEDI LiDAR waveforms with deep ensembles," *Remote Sensing of Environment*, 268, 112760. 2022.
- [11] T.J. Schmugge & T.J. Jackson, "A dielectric model of the vegetation effects on the microwave emission from soils," *IEEE Transactions on Geoscience and Remote Sensing*, 30(4), pp. 757 – 760. 1992.
- [12] D. Chaparro, T. Jagdhuber, M. Piles, D. Entekhabi, F. Jonard, A. Fluhner, ... & A. Camps, "Global L-band vegetation volume fraction estimates for modeling vegetation optical depth," *IGARSS 2021*, IEEE, pp. 6399-6402. 2021.
- [13] F.T. Ulaby, M.A. El-Rayes, "Microwave dielectric spectrum of vegetation – part II: dual dispersion model," *IEEE TGRS*, Ge-25(5), pp. 550–557. 1987.
- [14] Z. Li, J. Zeng, Q. Chen & H. Bi, "The measurement and model construction of complex permittivity of vegetation," *Science China Earth Sciences*, 57(4), pp. 729-740. 2014.
- [15] M. Yebra, G. Scortechini, A. Badi, M.E. Beget, M.M. Boer, R. Bradstock, ... & S. Ustin, "Globe-LFMC, a global plant water status database for vegetation ecophysiology and wildfire applications," *Scientific Data*, 6(1), pp. 1-8. 2019.
- [16] A. G. Konings, K. Rao & S. C. Steele-Dunne. "Macro to micro: microwave remote sensing of plant water content for physiology and ecology," *New Phytologist*, 223(3), 1166-1172. 2019.
- [17] ESA. Land Cover CCI Product User Guide Version 2. Tech. Rep. (2017). Available at: maps.elie.ucl.ac.be/CCI/viewer/download/ESACCI-LC-h2-PUGv2_2.0.pdf
- [18] D. Chaparro, M. Piles, M. Vall-Llossera, A. Camps, A. G. Konings & D. Entekhabi, "L-band vegetation optical depth seasonal metrics for crop yield assessment," *Remote Sensing of Environment*, 212, pp. 249-259. 2018.
- [19] C. Olivares-Cabello, D. Chaparro, M. Vall-Llossera, A. Camps, C. López-Martínez, "Global unsupervised assessment of multifrequency vegetation optical depth to vegetation cover," *IEEE JSTARS*, 16, pp. 538-552. 2023.

5. ACKNOWLEDGEMENTS

The work of D. Chaparro was supported by the XXXIII Ramón Areces Postdoctoral Fellowship, and by "la Caixa" Foundation (ID 100010434) under Grant LCF/PR/MIT19/51840001 (MIT-Spain Seed Fund). This research was supported also by the Spanish Ministry of Science and Innovation (MCIN/AEI /10.13039/501100011033), through the coordinated project INTERACT PID2020-114623RB-C32. M. Piles thanks the support of Conselleria de Innovación, Universidades, Ciencia y Sociedad Digital through the project AI4CS CIPROM/2021/56.